Supplementary Materials

Genetic Loss of Insulin Receptors Worsens Cardiac Efficiency in Diabetes

Heiko Bugger[1], Christian Riehle[1], Bharat Jaishy[1], Adam R. Wende[1], Joseph Tuinei[1], Dong Chen[3,4], Jamie Soto[1], Karla M. Pires[1], Sihem Boudina[1], Heather A. Theobald[1], Ivan Luptak[5], Benjamin Wayment[2], Xiaohui Wang[2], Sheldon E. Litwin[2], Bart C. Weimer[3,4], and E. Dale Abel

Gene Expression: Total RNA was extracted from hearts with Trizol reagent (Invitrogen Corporation, Carlsbad, CA), purified with the RNEasy Kit (Qiagen Inc., Valencia, CA) and reverse transcribed [1]. Equal amounts of cDNA were subjected to quantitative real-time RT-PCR using SYBR Green as a probe. Data were normalized by expressing them relative to the levels of the invariant transcript 16S RNA. Primer sequences are presented in Supplementary Table 1.

Comparative mitochondrial proteomics: Cardiac mitochondria were isolated, purified and fractionated into matrix and membrane fractions, as described previously [2, 3]. 5µl of 0.2% RapidGest (Waters, Manchester, UK) was added to 20µg of matrix or membrane protein sample in 15µL H_2O. The mixed solution was heated at 80°C for 20min, and the protein mixtures were then tryptically digested according to a modified digestion method in the Waters Protein Expression System Manual (Waters, 2006). After adding NH_4HCO_3 and treating with dithiothreitol and iodoacetamide, 4µL of 0.11µg/µL trypsin in 25mmol/L NH_4HCO_3 was added to the protein sample. Samples were incubated at 37°C overnight, incubated with 1% formic acid for 30 minutes at 37°C, and centrifuged at 10,000xg for

10min. The supernatant was analyzed by LC-MS/MS. Equal amounts of digested protein were introduced into a Symmetry® C18 trapping column (180µmol/L x 20mm) by NanoACQUITY Sample Manager (Waters, Manchester, UK) and washed with H_2O for 2min at 10mL/min. Using solvent A (99.9% H_2O and 0.1% formic acid) and solvent B (99.9% acetonitrile and 0.1% formic acid), the peptides were eluted from the trapping column over a 100µm x 100mm BEH 130 C18 column with a 140min gradient (1-4% B for 0.1min, 4-25% B for 89.9min, 25-35% B for 5min, 35-85% B for 2min, 85% B for 13min, 85-95% B for 8min, 95-1% B for 2min and 1% B for 20min) at 0.8µL/min flow rate using an NanoACQUITY UPLC (Waters, Manchester, UK). The mass spectrometer, Q-TOF Premier (Waters, Manchester, UK), was set to a parallel fragmentation mode (MSE) with scan times of 1.0 second. The low fragmentation energy was 5 volts and the high fragmentation ranged from 17 to 45 volts. (GLU1)-Fibrinopeptide B was used as an external calibration standard with LockSpray. Enolase was used as the spiked control. Mass spectrometry data were analyzed by Waters ProteinLynx Global Server (PLGS) 2.3. The following default setting was used for protein identification. Minimum Peptide Matches Per Protein: 1, Minimum Fragment Ion Matches Per Peptide: 3, Minimum Fragment Ion Matches Per Protein: 7 and the protein False Positive Discovery Rate: 4%. Canonical pathway analysis was performed using the Ingenuity Pathways Analysis (IPA) software (Redwood City, CA).

Staining for 4-hydroxy-2-nonenal (HNE): Mouse monoclonal anti-HNE antibody (Oxis International, Portland, OR) was used to detect lipid peroxidation of left ventricular sections. Biotin-conjugated anti-mouse IgG (Vector Laboratories, Burlingame, CA) was utilized as secondary antibody. The immunoreaction was visualized by using Vectastain AP SK 5000 alkaline phosphatase kit (Vector Laboratories, Burlingame, CA) and permanently mounted. Ten color images of HNE staining were selected from three sections of the heart and viewed at × 200 magnification. The area and intensity of staining were scored by four independent

blinded observers for semiquantification. The scoring range was the following: 0, no visible staining; 1, faint staining; 2 mild staining, 3 moderate staining; and 4, strong staining, as reported previously [4].

Echocardiography: Transthoracic echocardiography was performed as previously described [2]. Briefly, images were taken in mice lightly anesthetized with avertin (0.2 ml/10 g body weight). Limb leads were attached for electrocardiogram gating, and the animals were imaged in the supine position with a 13-MHz linear probe (Vivid FiVe; GE Medical Systems, Milwaukee, Wisconsin, USA). Two-dimensional guided M-mode images were taken in both short and long axis projections.

Akt phosphorylation: For evaluation of insulin-mediated Akt activation, mice were anesthetized and injected with saline or 0.01 U Insulin via the inferior vena cava after a six-hour fast, after which the heart was rapidly excised and flash frozen in liquid nitrogen 5 min post injection. Heart lysates were then subjected to western blot analysis using antibodies that recognize total Akt (Cell signaling, Danvers, MA, 1:2000/1:2000) and phospho-Akt (Ser^{473}) (Millipore, Billerica, MA, 1:1000/1:1000).

Tissue glycogen content: Glycogen concentrations in heart tissue extracts were measured as described [5]. Briefly, heart tissues were flash-frozen and homogenized in 0.3 M perchloric acid. The extract was assayed in a buffer containing 50 mM Na acetate and 0.02% bovine serum albumin with or without α-amyloglucosidase (A7420, Sigma, St. Louis MO). Changes in absorption at 340 nM were compared with a glucose standard of 0 to 80 μmol. Data were expressed as glucose released from glycogen normalized to tissue weight.

References

[1] Bugger H, Boudina S, Hu XX, Tuinei J, Zaha VG, Theobald HA, et al. Type 1 diabetic akita mouse hearts are insulin sensitive but manifest structurally abnormal mitochondria that remain coupled despite increased uncoupling protein 3. Diabetes. 2008;57:2924-32.

[2] Boudina S, Bugger H, Sena S, O'Neill BT, Zaha VG, Ilkun O, et al. Contribution of impaired myocardial insulin signaling to mitochondrial dysfunction and oxidative stress in the heart. Circulation. 2009;119:1272-83.

[3] Bugger H, Chen D, Riehle C, Soto J, Theobald HA, Hu XX, et al. Tissue-specific remodeling of the mitochondrial proteome in type 1 diabetic akita mice. Diabetes. 2009;58:1986-97.

[4] Qin F, Simeone M, Patel R. Inhibition of NADPH oxidase reduces myocardial oxidative stress and apoptosis and improves cardiac function in heart failure after myocardial infarction. Free Radic Biol Med. 2007;43:271-81.

[5] Wende AR, Schaeffer PJ, Parker GJ, Zechner C, Han DH, Chen MM, et al. A role for the transcriptional coactivator PGC-1alpha in muscle refueling. J Biol Chem. 2007;282:36642-51.

Supplementary Figure legends

Supplementary Figure 1: Cardiac glycogen levels. 2-way ANOVA was performed to analyze differences by treatment and genotype. Cardiac glycogen levels ($p<0.05$ for treatment, and interaction of genotype and treatment) of non-diabetic WT and CIRKO respectively (WT–Veh, CIRKO–Veh), WT–STZ, and CIRKO–STZ mice; n=4-5. Bonferroni: * $p<0.05$ for WT-Veh vs. WT-STZ and CIRKO-STZ respectively, and # $p<0.05$ for CIRKO-Veh vs. WT-STZ and CIRKO-STZ respectively.

Supplementary Figure 2: Insulin-stimulated Akt phosphorylation is maintained in insulin-deficient WT-STZ mice. 2-way ANOVA was performed to analyze differences by treatment and genotype. (A) Representative images of Akt phosphorylation at Ser^{473} and of total Akt in the presence or absence of insulin, and (B) quantification of the ratio of phosphorylated Akt to total Akt ($p<0.05$ for insulin treatment); n=3-6.

Supplementary Figure 3: Cellular 4-hydroxynonenal (HNE) levels. 2-way ANOVA was performed to analyze differences by treatment and genotype, including a Bonferroni post-hoc analysis. (A) Representative images of HNE staining of left ventricular sections, and (B) quantification of HNE levels of non-diabetic WT and CIRKO (WT–Veh, CIRKO–Veh) respectively, WT–STZ, and CIRKO–STZ mice ($p<0.05$ for genotype, treatment, and their interaction; Bonferroni: * $p<0.05$ for WT-STZ vs. all other groups respectively); n=4-9

Supplementary Figure 4: Myocardial expression of fatty acid oxidation genes. 2-way ANOVA was performed to analyze differences by treatment and genotype. Myocardial expression of PPARα, Cpt1b ($p<0.05$ for treatment), Cpt2 ($p<0.05$ for genotype), MCAD ($p<0.05$ for genotype), LCAD ($p<0.05$ for treatment), Acaa2 ($p<0.05$ for genotype and treatment), Hadhb, and MTE1 ($p<0.05$ for treatment), normalized to 16S RNA transcript levels. Values represent fold change in mRNA transcript levels relative to WT–Veh, which was assigned as one (dashed line); n=5-8.

Supplementary Figure 5: Myocardial expression of genes encoding for proteins regulating glucose utilization and mitochondrial biogenesis, and of OXPHOS genes. 2-way ANOVA was performed to analyze differences by treatment and genotype. Myocardial gene expression of Pdk4, PdhA1 ($p<0.05$ for treatment), PGC-1α, Ndufa9, Uqcrc-1, Cox4i

($p<0.05$ for genotype), and ATPase6 ($p<0.05$ for genotype), normalized to 16S RNA transcript levels. Values represent fold change in mRNA transcript levels relative to WT–Veh, which was assigned as one (dashed line); n=5-8

Supplementary Table 1: Primer sequences and accession numbers of genes used for quantification of mRNA levels by real-time RT-PCR.

Gene	Forward/Reverse primer sequences	Accession number
Peroxisome proliferator activated receptor α (PPARα)	GAGAATCCACGAAGCCTACC AATCGGACCTCTGCCTCTTT	NM_011144
Carnitine palmitoyltransferase 1b (CPT1b)	TGCCTTTACATCGTCTCCAA AGACCCCGTAGCCATCATC	NM_009948
Carnitine palmitoyltransferase 2 (CPT2)	CCAGCTGACCAAAGAAGCA GCAGCCTATCCAGTCATCGT	NM_009949
Acyl-Coenzyme A dehydrogenase, medium chain (MCAD)	ACTGACGCCGTTCAGATTTT GCTTAGTTACACGAGGGTGATG	NM_007382
Acyl-Coenzyme A dehydrogenase, long chain (LCAD)	ATGGCAAAATACTGGGCATC TCTTGCGATCAGCTCTTTCA	NM_007381
Acetyl-Coenzyme A acyltransferase 2 (Acaa2)	CAGCGAAGATGCTGTCAAAA GACACGAAGTAGCCCACGAC	NM_177470
Hydroxyacyl-Coenzyme A dehydrogenase/3-ketoacyl-Coenzyme A thiolase/enoyl Coenzyme A hydratase (trifunctional protein), subunit b (Hadhb)	GCCAACAGACTGAGGAAGGA ACACTGGCAAGGCTGGATT	NM_145558
Pyruvate dehydrogenase kinase, isoenzyme 4 (Pdk4)	GCTTGCCAATTTCTCGTCTC CTTCTCCTTCGCCAGGTTCT	NM_013743
Pyruvate dehydrogenase E1 alpha 1 (PDHA1)	GGGACGTCTGTTGAGAGAGC TGTGTCCATGGTAGCGGTAA	NM_008810
Peroxisome proliferator activated receptor γ co-activator 1α (PGC-1α)	ACTGAGCTACCCTTGGGATG TAAGGATTTCGGTGGTGACA	NM_008904
NADH dehydrogenase (ubiquinone) 1 alpha subcomplex 9 (Ndufa9)	ATCCCTTACCCTTTGCCACT CCGTAGCACCTCAATGGACT	NM_025358
Ubiquinol-cytochrome c reductase core	TGCCAGAGTTTCCAGACCTT	NM_025407

protein 1 (Uqcrc1)	CCAAATGAGACACCAAAGCA	
Cytochrome c oxidase subunit IV isoform 1 (COX4i)	CGCTGAAGGAGAAGGAGAAG GCAGTGAAGCCAATGAAGAA	NM_009941
ATPase 6, mitochondrial (ATPase6)	CAAACAAATAATGCTAATCCACACACC GCTGTAAGCCGGACTGCTAATG	NC_005089.1
Uncoupling protein 2 (UCP2)	TCTCCTGAAAGCCAACCTCA CTACGTTCCAGGATCCCAAG	NM_011671
Uncoupling protein 3 (UCP3)	TGCTGAGATGGTGACCTACGA CCAAAGGCAGAGACAAAGTGA	NM_009464
Mitochondrial acyl-CoA thioesterase 1 (MTE1)	GACCTCCCCAAGAGCATAGA TCCTTGTAGGAGATGGTGTTCC	NM_134188
solute carrier family 25 (mitochondrial carrier, adenine nucleotide translocator 1), member 4 (Slc25a4) (ANT1)	AGGGTCTCTACCAGGGTTTCA TCACACTCTGGGCAATCATC	NM_007450

Supplementary Table 2: Heart weight-to-body weight ratios and heart weight-to-tibia length ratios at 12 weeks of age.

	WT-Veh (15)	CIRKO-Veh (15)	WT-STZ (15)	CIRKO-STZ (15)
Heart weight [mg] * #	109.6 ± 3.3	86.4 ± 2.9	98.4 ± 3.2	80.8 ± 2.6
Body weight [g] #	26.6 ± 0.9	25.2 ± 0.9	23.5 ± 0.7	21.9 ± 0.7
Tibia length [mm]	17.2 ± 0.1	16.9 ± 0.2	16.8 ± 0.1	17.0 ± 0.1
HW-BW ratio [mg/g] *	4.1 ± 0.1	3.5 ± 0.1	4.2 ± 0.1	3.7 ± 0.1
HW-TL-ratio [mg/mm] * #	6.4 ± 0.2	5.1 ± 0.1	5.8 ± 0.2	4.8 ± 0.1

2-way ANOVA was performed to analyze differences by treatment and genotype.

Effect of treatment ($p<0.05$)

* Effect of genotype ($p<0.05$)

Supplementary Table 3 : Echocardiographic parameters at 12 weeks of age.

	WT-Veh (6)	CIRKO-Veh (6)	WT-STZ (5)	CIRKO-STZ (8)
IVSd [cm] *	0.064 ± 0.004	0.046 ± 0.003	0.063 ± 0.003	0.043 ± 0.003
IVSs [cm] *	0.106 ± 0.004	0.076 ± 0.005	0.099 ± 0.006	0.076 ± 0.003
LVIDd [cm] #	0.389 ± 0.005	0.391 ± 0.009	0.350 ± 0.013	0.367 ± 0.007
LVIDs [cm]	0.265 ± 0.011	0.283 ± 0.011	0.254 ± 0.016	0.254 ± 0.008
LVPWd [cm]	0.072 ± 0.004	0.066 ± 0.009	0.070 ± 0.005	0.074 ± 0.006
LVPWs [cm]	0.102 ± 0.007	0.091 ± 0.006	0.089 ± 0.007	0.107 ± 0.006
HR [bpm]	452 ± 19	446 ± 25	447 ± 25	401 ± 28
EF [%]	67.6 ± 3.3	62.0 ± 2.5	62.1 ± 3.3	66.4 ± 2.2
FS [%]	31.7 ± 2.5	27.7 ± 1.6	27.9 ± 2.1	30.7 ± 1.5
SV [µl] #	40 ± 3	36 ± 3	30 ± 2	33 ± 2
CO [ml/min] #	18.2 ± 1.8	16.0 ± 1.7	13.3 ± 0.7	13.5 ± 1.3
BW [g] #	26.1 ± 0.5	25.5 ± 0.8	23.4 ± 0.4	22.3 ± 0.5
SV/BW [µl/g]	1.53 ± 0.12	1.39 ± 0.08	1.28 ± 0.06	1.50 ± 0.10
CO/BW [ml/min/g]	0.70 ± 0.07	0.63 ± 0.06	0.57 ± 0.04	0.61 ± 0.06

2-way ANOVA was performed to analyze differences by treatment and genotype.

Effect of treatment ($p<0.05$)

* Effect of genotype ($p<0.05$)

Supplementary Table 4: Mitochondrial abundance of proteins involved in fatty acid oxidation, citrate cycle, pyruvate decarboxylation, oxidative phosphorylation, and adenine nucleotide translocation in hearts from CIRKO – Veh, WT – STZ, and CIRKO – STZ mice, presented as fold change relative to WT-Veh. * indicates decreased abundance vs. WT-Veh ($p<0.05$); # indicates increased abundance vs. WT-Veh ($p<0.05$).

	CIRKO–Veh	WT–STZ	CIRKO–STZ
Fatty acid oxidation (membrane fraction)			
acetyl-Coenzyme A acyltransferase 2	0.86 *	1.49 #	1.10
acetyl-Coenzyme A dehydrogenase, long-chain	0.99	1.28 #	1.15 #
acetyl-Coenzyme A dehydrogenase, medium chain	1.06	1.33 #	1.11 #
acyl-Coenzyme A dehydrogenase, very long chain	0.83 *	1.02	1.12 #
carnitine palmitoyltransferase 1b, muscle	0.85 *	0.88 *	1.02
carnitine palmitoyltransferase 2	0.68 *	1.04	0.94
dodecenoyl-Coenzyme A delta isomerase	0.86	1.43 #	1.25 #
electron transferring flavoprotein, alpha polypeptide	0.99	1.32 #	1.11
electron transferring flavoprotein, beta polypeptide	1.03	1.28 #	1.12 #
electron transferring flavoprotein, dehydrogenase	0.82 *	1.10 #	0.96
enoyl Coenzyme A hydratase, short chain, 1, mitochondrial	1.10	1.02	0.87
hydroxyacyl-Coenzyme A dehydrogenase, alpha subunit	0.88 *	1.27 #	1.11 #
hydroxyacyl-Coenzyme A dehydrogenase, beta subunit	0.90 *	1.19 #	1.03
Citrate cycle (matrix fraction)			
aconitase 2, mitochondrial	0.98	1.02	0.95 *
citrate synthase	0.99	1.05 #	1.04
fumarate hydratase 1	0.79 *	0.76 *	0.72 *
isocitrate dehydrogenase 3 (NAD+) alpha	0.83 *	0.86 *	0.74 *
malate dehydrogenase 2, NAD (mitochondrial)	1.04	0.93 *	0.84 *
oxoglutarate dehydrogenase (lipoamide)	0.93	0.82 *	0.87 *
succinate dehydrogenase Fp subunit	0.98	1.04	1.03
succinate dehydrogenase Ip subunit	0.84 *	0.87 *	0.92
Pyruvate decarboxylation			

pyruvate dehydrogenase (lipoamide) beta	0.95	0.89	0.88 *
pyruvate dehydrogenase E1 alpha 1	0.93	0.83 *	0.93
Oxidative phosphorylation (membrane fraction)			
Complex I			
NADH dehydrogenase (ubiquinone) 1 alpha subcomplex 10	1.09	1.06	1.14
NADH dehydrogenase (ubiquinone) 1 alpha subcomplex, 13	0.90	0.93	0.96
NADH dehydrogenase (ubiquinone) 1 alpha subcomplex, 4 [	0.83 *	0.88 *	0.93
NADH dehydrogenase (ubiquinone) 1 alpha subcomplex, 5	0.86	0.94	0.88
NADH dehydrogenase (ubiquinone) 1 alpha subcomplex, 8	0.94	0.92	1.01
NADH dehydrogenase (ubiquinone) 1 alpha subcomplex, 9	1.04	1.01	1.11
NADH dehydrogenase (ubiquinone) 1 beta subcomplex, 10	0.93	0.85	1.15
NADH dehydrogenase (ubiquinone) 1 beta subcomplex, 9	0.90	0.97	0.98
NADH dehydrogenase (ubiquinone) 1, subcomplex unknown, 2	1.04	0.96	0.98
NADH dehydrogenase (ubiquinone) Fe-S protein 1	1.08	0.88 *	1.01
NADH dehydrogenase (ubiquinone) Fe-S protein 2	0.88	0.80 *	0.85 *
NADH dehydrogenase (ubiquinone) Fe-S protein 3	0.95	0.70 *	0.88 *
NADH dehydrogenase (ubiquinone) Fe-S protein 4	1.19	0.93	1.01
NADH dehydrogenase (ubiquinone) Fe-S protein 6	1.02	0.98	1.06
NADH dehydrogenase (ubiquinone) Fe-S protein 7	0.86	0.78 *	0.97
NADH dehydrogenase (ubiquinone) flavoprotein 1	0.94	0.97	1.10
NADH dehydrogenase 1 beta subcomplex 4	1.04	0.90	1.00
Complex II			
succinate dehydrogenase Fp subunit	0.98	1.04	1.03
succinate dehydrogenase Ip subunit	0.84 *	0.87 *	0.92
Complex III			
ubiquinol cytochrome c reductase core protein 2	1.05	1.01	1.02
ubiquinol-cytochrome c reductase binding protein	1.02	1.00	0.96
ubiquinol-cytochrome c reductase core protein 1	0.93 *	0.90 *	0.99
ubiquinol-cytochrome c reductase, Rieske iron-sulfur polypeptide 1	0.93	0.93	0.95
Complex IV			
cytochrome c oxidase subunit II	0.83 *	1.06	0.98
cytochrome c oxidase subunit IV isoform 1	1.02	0.95	1.06

cytochrome c oxidase, subunit Va	0.93	0.92	0.98
cytochrome c oxidase, subunit Vb	1.05	1.05	1.12
cytochrome c oxidase, subunit VIb polypeptide 1	0.86 *	0.93	1.05
cytochrome c oxidase, subunit VIc	1.02	1.00	1.04
cytochrome c oxidase, subunit VIIa 1	0.75 *	0.86	0.75
Complex V			
ATP synthase, mitochondrial F1 complex, beta subunit	0.88 *	0.94 *	0.95 *
ATP synthase, mitochondrial F0 complex, subunit b, isoform 1	1.05	1.06	1.18 #
ATP synthase, mitochondrial F0 complex, subunit d	1.05	1.08	1.06
ATP synthase, mitochondrial F0 complex, subunit F	1.03	0.89	0.98
ATP synthase, mitochondrial F0 complex, subunit f, isoform 2	0.95	0.88	0.90
ATP synthase, mitochondrial F1 complex, alpha subunit, isoform 1	0.95 *	0.98	1.05 #
ATP synthase, mitochondrial F1 complex, delta subunit precursor	0.92	0.80 *	0.88 *
ATP synthase, mitochondrial F1 complex, gamma subunit	0.94	1.10	1.00
ATP synthase, mitochondrial F1 complex, O subunit	0.90 *	0.98	0.93
Other			
cytochrome c-1	0.88	0.95	1.00
hypothetical protein LOC66152	0.74 *	0.80 *	0.79 *
low molecular mass ubiquinone-binding protein	0.88	0.99	0.86
Adenine nucleotide translocases			
PREDICTED: similar to ADP/ATP translocase 1 (Adenine nucleotide translocator 1) (ANT 1) (ADP,ATP carrier protein 1) (Solute carrier family 25 member 4) (ADP,ATP carrier protein, heart/skeletal muscle isoform T1) (mANC1) isoform 2	1.06 #	0.93 *	0.96
PREDICTED: similar to ADP/ATP translocase 2 (Adenine nucleotide translocator 2) (ANT 2) (ADP,ATP carrier protein 2) (Solute carrier family 25 member 5) isoform 1	1.18 #	1.02	0.93

Supplementary Figure 1

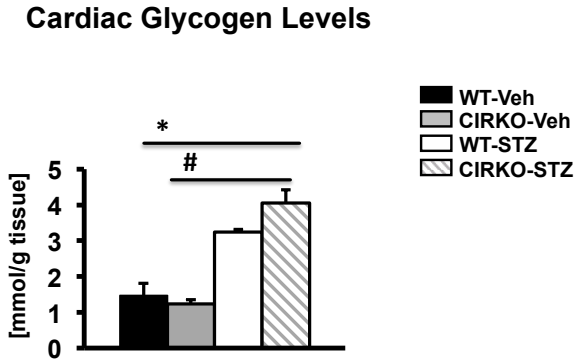

Supplementary Figure 2

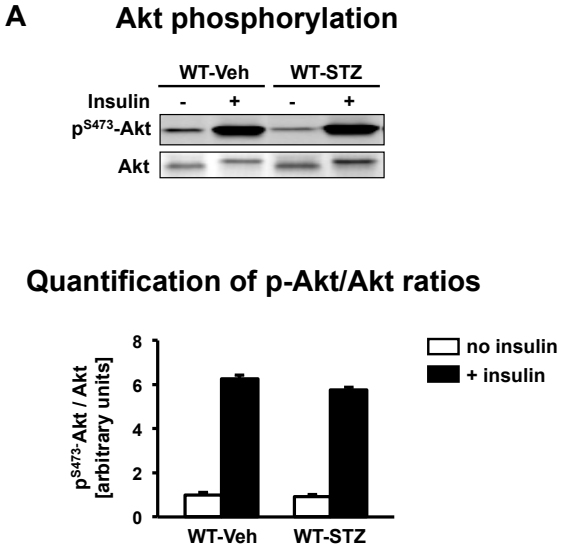

Supplementary Figure 3

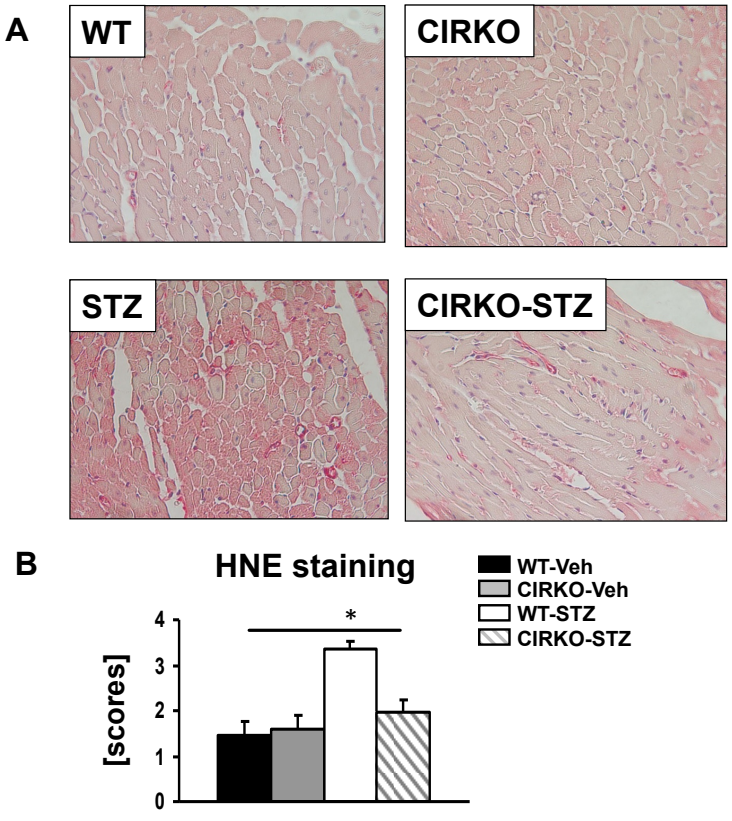

Supplementary Figure 4

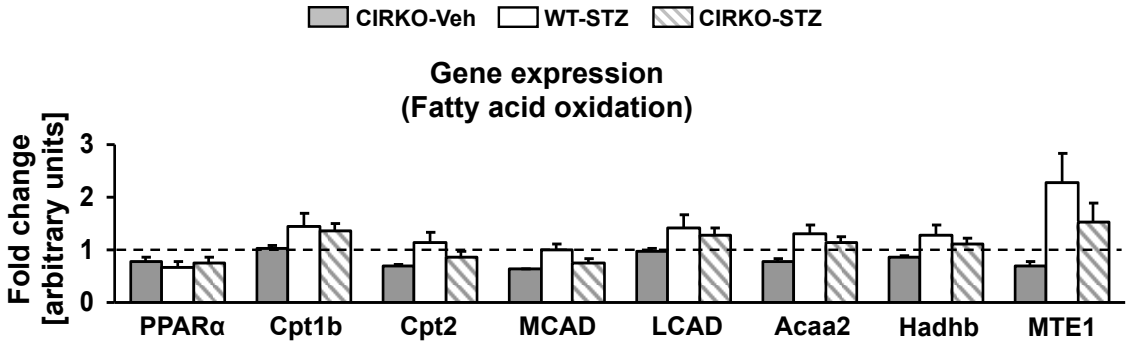

Supplementary Figure 5